Finite Element Modeling Simulation of In-Plane Forming Limit Diagrams of Sheets Containing Finite Defects

K. NARASIMHAN and R.H. WAGONER

Finite element modeling (FEM) has been used to predict forming limit diagrams (FLDs) of thin sheets based on two-dimensional (2-D) finite thickness defects. The local growth of these defects is simulated until an arbitrary failure criterion is reached. Many aspects of this simulation reproduce the standard Marciniak-Kuczynski (M-K) results. For example, the plane strain intercept, FLD_0, is sensitive to the material work hardening, n, and the strain rate sensitivity, m, but is not affected by the normal anisotropy, r. The positive side of the FLD was characterized by a line of logarithmic slope P. The value of P decreases sharply as n and m increase. The effect of r depends on the choice of yield function. The absolute location of the FLD, as given by the FLD_0, depends not only on the material properties, but also on the choice of failure criterion, defect geometry, and details of the simulative model (mesh size, number of defect dimensions, *etc.*). This is true of any measurement or simulation of the FLDs. Therefore, we propose that the FLD_0 be used as the single "fitting parameter" between modeling and experimental results: a more realistic approach based on what is actually measured in the FLD experiments. This method allows clarification of the role of material plasticity properties (*e.g.*, n, m, and r) *vs* fracture properties (contained in the FLD_0) in determining the shape of the FLDs.

I. INTRODUCTION

FLOW localization during sheet stretching limits metal formability. A sheet necks and eventually fails in locations where critical limit strains are exceeded. A representation of all combinations of such critical major and minor strains gives rise to a forming limit diagram (FLD). The concept of forming limits was first introduced by Keeler and Backofen[1] and Keeler,[2,3] and the standard form of the FLD was later presented by Goodwin.[4] Hecker[5] presented a detailed procedure to measure the FLD from large negative to large positive minor strains. Azrin and Backofen[6] introduced a new testing technique to determine the in-plane FLD. The current state of art on both the experimental and theoretical FLDs is reviewed in a recent book edited by Wagoner *et al.*[7]

Theoretical calculations of the FLDs were initially based on Hill's criterion for localized necking along a direction of zero extension.[8] Hill's criterion does not allow for localized necking of materials with smooth yield surfaces under biaxial stretching ($\varepsilon_2 > 0$) conditions. Marciniak and Kuczynski (M-K)[9] and Marciniak *et al.*,[10] by introducing a thickness imperfection of infinite length normal to the principal stress, developed the first analytical model to predict localized necking in biaxial stretching of sheets. They showed that the presence of even slight intrinsic inhomogeneities in load bearing capacity throughout a deforming sheet can lead to unstable growth of strain in the weaker regions and subsequently lead to localized necking and failure. Since then, several researchers have used M-K analysis to predict localized necking during biaxial stretching (with $\varepsilon_2 > 0$). The variants of M-K analysis for predicting localized necking have been reviewed in the past.[11,12,13]

In establishing the original theory, M-K[9] considered a material element with uniform mechanical properties but with a notch in thickness extending across it, along the minor principal stress direction, X_2, as represented in Figure 1. The geometrical notch serves as a mechanical analog for a hypothesized initial local weakness. The ratio of the thickness of the notch to that of the bulk was defined as the weakness factor, f.

$$f = \frac{\text{thickness of notch}}{\text{thickness of bulk}} \qquad [1]$$

The source of an intrinsic inhomogeneity in a real material is not clear, but suggestions have been made relating it to material property variations,[10] local prestrains, thermal notches, and thickness variations.[14] In real sheet forming applications, strain localization can be initiated and developed without material or thickness inhomogeneities. Friction and contact conditions existing during the sheet forming control the development of nonuniform strain distribution and the eventual strain localization process, leading to splitting failures. Such a process is only approximately modeled by in-plane representations like the M-K or the finite element modeling (FEM) approach presented here, and the complex boundary conditions initiating the localization process are usually contained in a single parameter of unknown origin, such as the weakness factor, f, in Eq. [1].

In the M-K theory, instability is viewed as a process in which the strain state in a region of local weakness evolves to one of plane strain as deformation proceeds uniformly in the bulk. While this characteristic agrees with that observed for many sheet failures, the M-K analysis is based on an unrealistically simple model. The M-K defect (Figure 1) is infinite in length, with no end

K. NARASIMHAN, Postdoctoral Researcher, and R.H. WAGONER, Professor, are with the Department of Materials Science and Engineering, The Ohio State University, Columbus, OH 43210.

Manuscript submitted November 2, 1990.

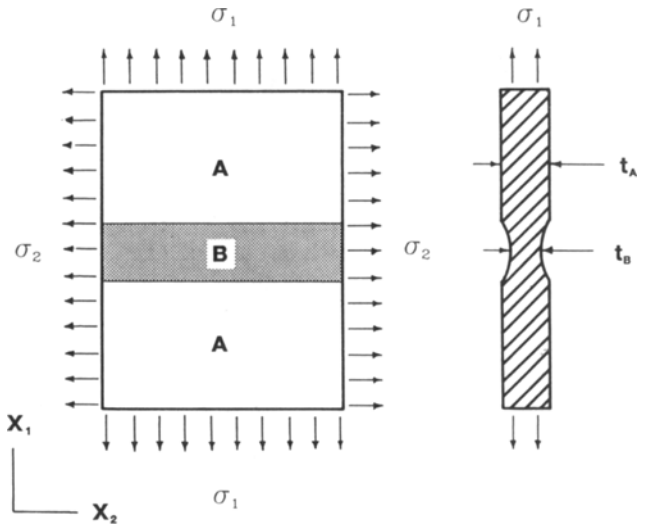

Fig. 1 — Schematic of the M-K model for a sheet element "A" with a thickness inhomogeneity "B" aligned parallel to the minor stress axis, x_2.[9]

effects taken into account; such defects do not exist in real sheet materials. The M-K analysis, therefore, implicitly imposes nonphysical boundary conditions by way of the uniform minor strains throughout the sheet sample. These two simplifications allow the closed form one-dimensional (1-D) solutions (that is, those which allow variations in field quantities in one direction only) that M-K sought but overstate the impact of a real material defect. Finite element modeling allows relaxation of these two restricting assumptions by solving for nonuniform internal stresses and strains under prescribed displacement boundary conditions. Bate and Wilson[15] used FEM to analyze the development of strain localization in a biaxially stretched sheet of work-hardening material which contained a regular array of interacting, axisymmetric defects. They consider, in detail, the effect of shape and distribution of the defects on strain localization and FLDs. They have also shown that in the case of finite (compact) defects, the magnitude of strains within the finite defect can be much larger than within the M-K defect so that failure may, in fact, occur by fracture inside the defect rather than by flow localization. In this paper, we consider the effect of material parameters on the FLD_0 and shape of the FLD.

More than 80 pct of industry failures occur near plane strain conditions.[16] Therefore, the limit strain in plane strain conditions (FLD_0) is the quantity usually sought in experiments. It is possible to "predict" the experimentally observed FLD_0 by a suitable choice of the weakness factor, f. In fact, since f has an unknown physical meaning, it is simply a fitting parameter that allows a model to predict the experimentally measured FLD_0. The choice of f depends on the details of the model and the material. Therefore, it is not meaningful to identify f with specific material characteristics.

This paper analyzes the development of in-plane strain localization in sheets containing isolated, noninteracting finite defects. The analysis is based on a two-dimensional (2-D) rigid viscoplastic FEM program with deformation imposed by displacement boundary conditions remote from the defect. Necking during biaxial stretching is simulated automatically, and failure is declared using three failure criteria. The analysis improves on M-K analysis in three ways: (1) introduces finite-extent defects which are more physically reasonable; (2) eliminates the uniform-minor strain boundary conditions; and (3) allows variations of field quantities in two principal directions. However, the need for a single fitting parameter cannot be avoided. The sensitivity of the predicted FLD on the work-hardening exponent (n), strain-rate sensitivity (m), and anisotropy parameter (r) is calculated. The FEM results are compared to the predictions obtained from the M-K analysis. A new framework for understanding and analyzing FLDs is proposed.

II. FINITE ELEMENT MODEL

The finite element program was developed on the basis of rigid viscoplastic theory for in-plane deformation under plane-stress conditions[17] using a formulation presented by Wang.[18] Constant strain triangular elements are used. This program has been used to analyze sheet tensile necking,[19,20] and three-dimensional (3-D) membrane versions have been developed[21,22] to analyze sheet stamping operations. Other effects, such as non-isothermality, have also been introduced into the in-plane[23,24] and 3-D versions[25] of the FEM program. A brief review of the program features and the application to biaxial forming limit is presented next.

The work-hardening and strain rate sensitivity models incorporated in the present analysis may be expressed as follows:

$$\bar{\sigma} = k(\bar{\varepsilon}_0 + \bar{\varepsilon})^n \left[\frac{\dot{\bar{\varepsilon}}}{\dot{\bar{\varepsilon}}_0}\right]^m \qquad [2]$$

In Eq. [2], the parameters represent effective stress ($\bar{\sigma}$), strength coefficient (k), effective strain ($\bar{\varepsilon}$), prestrain ($\bar{\varepsilon}_0$), strain-hardening exponent (n), current effective strain rate ($\dot{\bar{\varepsilon}}$), reference effective strain rate ($\dot{\bar{\varepsilon}}_0$), and strain rate sensitivity index (m).

Currently, effective stress and strain may be defined by either Hill's nonquadratic yield theory[26] for normal anisotropy or Hosford's nonquadratic yield theory[27] for normal anisotropy. More standard yield functions, such as the von Mises[28] or Hill's quadratic theory,[29] are subsets of both Hill's and Hosford's nonquadratic theories and are, therefore, immediately available in the program. The quantities for both nonquadratic theories are defined in terms of principal stresses and strain increments.

For Hill's[26] theory, they are given by

$$\bar{\sigma} = \left\{\frac{1}{2(1+r)}\left[(1+2r)\,|\sigma_1 - \sigma_2|^M + |\sigma_1 + \sigma_2|^M\right]\right\}^{1/M} \qquad [3]$$

$$d\bar{\varepsilon} = \frac{[2(1+r)]^{1/M}}{2}\left[\frac{1}{(1+2r)^{(1/(M-1))}}\,|d\varepsilon_1 - d\varepsilon_2|^{M/(M-1)} + |d\varepsilon_1 + d\varepsilon_2|^{M/(M-1)}\right]^{(M-1)/M} \qquad [4]$$

where the parameters M and r characterize the anisotropy of the yield surface. For the membrane formulation, σ_3 is identically zero. Substituting $M = 2$ and $r = 1$ in Eqs. [3] and [4] gives rise to the well-known von Mises[28] isotropic yield theory functions. With $M = 2$ and for any arbitrary r values, Eqs. [3] and [4] reduce to the 1948 Hill quadratic anisotropic yield theory.[29]

For Hosford's yield theory, effective stress is given by

$$\bar{\sigma} = \left\{ \frac{1}{(1+r)} \left[r|\sigma_1 - \sigma_2|^a + |\sigma_1|^a + |\sigma_1|^a + |\sigma_2|^a \right] \right\}^{1/a} \quad [5]$$

An explicit form for $d\bar{\varepsilon}$ does not exist but may be computed numerically.[30]

Hosford's yield function (Eq. [5]) also reduces to von Mises yield theory when $a = 2$ and $r = 1$ and to the 1948 Hill theory for $a = 2$ and arbitrary r. Based on crystallographical texture calculations for metals, the following values of a have been suggested: $a \simeq$ for body-centered cubic metals and $a \simeq 8 - 10$ for face-centered cubic metals.[27,31]

In the (2-D) version of the FEM program, inhomogeneities in material properties (*e.g.*, n, r, M, and $\bar{\varepsilon}_0$, as well as thickness) can be applied to any element or group of elements selected for evaluation. Relative variations in k (Eq. [2]) are equivalent to introducing proportional variations in thickness.

The majority of the calculations for predicting FLDs have been based on Hill's[29] 1948 quadratic, normal anisotropic yield theory (*i.e.*, $M = 2$ and $r \neq 1$). The incorporation of Hosford's theory into the FEM program is only a recent development.[29] As a consequence, only a limited number of predictions have been completed using Hosford's theory ($a = 6$).

Figure 2 shows a mesh representing one quadrant of a sheet containing a region of reduced thickness. The mesh consists of 946 constant strain triangular elements and 513 nodes. The shaded region in Figure 2 represents 72 elements of reduced thickness which form a notch with an aspect ratio of 1:1. The mesh shown in Figure 2 represents an optimized mesh. Preliminary studies showed that the FEM results were sensitive to some extent to the following two factors. (1) The ratio of the size of the notch to the size of the full mesh. In this regard, it was found that the FEM predicted results were consistent if the full mesh size was at least 7 times larger than the notch. The mesh used in this study has this ratio greater than 10, ensuring isolated-defect conditions for simulation purposes. (2) The number of elements present inside the notch. It was found that the FEM predicted consistent limit strains if at least 72 elements were present inside the notch. Defects with different aspect ratios were previously modeled by Burford and Wagoner.[32] They showed that the aspect ratio of the defect has a strong influence on the rate of strain localization (Figure 3) and thus on the predicted forming limit diagrams. For a fixed weakness factor of the defect ($f = 0.98$), the rate of strain localization is reduced by decreasing the aspect ratio of the defect, and the limit strains are correspondingly increased. Similarly, for a given aspect ratio of the

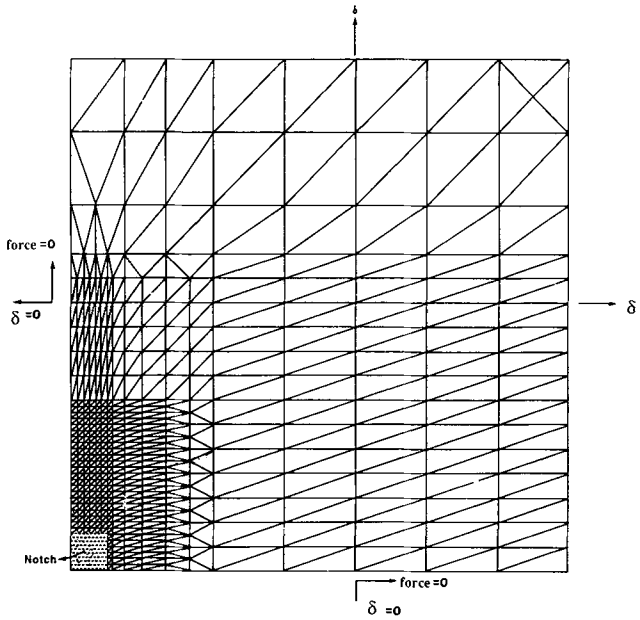

Fig. 2 — Undeformed finite element mesh, representing one quarter of the sheet. The shaded region represents the location of a thickness defect with an aspect ratio of 1:1.

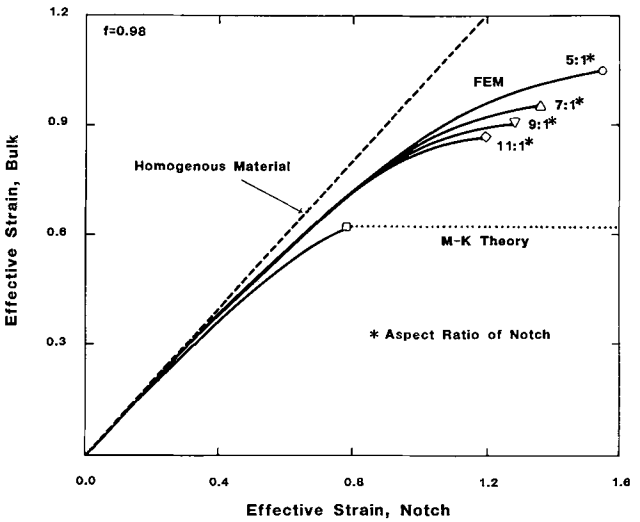

Fig. 3 — The effect of the aspect ratio of defect on strain localization: defects with larger aspect ratios localize strain rapidly.[32]

defect, they showed that a decrease in the magnitude of the weakness factor, f, increases the rate of strain localization, thus decreasing the corresponding limit strain.[32] In the present work, a thickness defect with an aspect ratio of 1:1 is used to maximize the differences between FEM and M-K analysis. The sensitivity of FLDs to n, m, and r is predicted using this 1:1 aspect ratio defect. Unless otherwise specified, the thickness defects are assumed to have a weakness factor, f, equal to 0.98.

The deformation is simulated by imposing displacement boundary conditions at the nodes along the boundaries of the mesh. Different strain paths can be simulated using different ratios of displacements between the two boundaries. For example, a balanced biaxial strain path

can be modeled by imposing equal displacements at all of the nodes present along both X^+ and Y^+ boundaries, with symmetry conditions imposed at X^- and Y^- boundaries (Figure 2). It is thus possible to simulate all of the strain paths in biaxial stretching.

III. FAILURE CRITERIA

During the simulation of biaxial stretching of sheet, strain gradients within the sample grow, eventually to produce large strains within the notch corresponding to the formation of a localized neck during the actual stretching of a sheet. In order to predict the limit strain, *i.e.*, the strain far removed from the notch when necking occurs, a failure criterion is required. A forming limit diagram can then be constructed by repeating the simulation for several strain paths and plotting the bulk strain when the failure criterion is reached.

In this study, three failure criteria were evaluated and compared. All of them are based on comparing the strain rate in the notch to that in the bulk, R.

The ratio of the major principal strain rate in the notch to that in the bulk, R_1, increases unstably during localized sheet stretching, as shown in Figure 4. The first criterion, based on major principal strain rate, is defined as follows:

$$R_1 = \frac{\text{major strain rate in the notch}}{\text{major strain rate in the bulk}} \geq 10.0 \qquad [6]$$

The ratio of the minor strain rate in the bulk to that in the notch, R_2, can also be used to describe flow localization. During initial stages of sheet stretching, this ratio is approximately equal to one, but at the onset of localized deformation, the ratio drastically increases, as shown in Figure 4. The second criterion examined takes the following form:

$$R_2 = \frac{\text{minor strain rate in the bulk}}{\text{minor strain rate in the notch}} \geq 10.0 \qquad [7]$$

This criterion corresponds to the notch attaining near plane strain path, similar to the original M-K criterion.

The third criterion is based on the scalar effective strain rates. Figure 4 shows that the ratio of the effective strain rate in the notch to that in the bulk R_3, exhibits a growth in slope at the onset of localized deformation. This criterion may be written as

$$R_3 = \frac{\text{effective strain rate in the notch}}{\text{effective strain rate in the bulk}} \geq 4.0 \qquad [8]$$

FLDs based on these three criteria showed little variance, typically less than 0.1 pct, in ε_2 for a given ε_1 (Figure 5). For the results presented in the remaining part of this paper, the R_3 criterion (Eq. [8]) was used.

IV. RESULTS AND DISCUSSION

Finite element modeling allows one to distinguish conveniently the influence of material parameters on the simulated FLDs. For example, the effects of the work-hardening exponent (n), strain rate sensitivity index (m), and anisotropy parameter (r) can easily be analyzed. The range of chosen material properties investigated represents the range of values commonly found in metals for sheet forming applications.[33] The FEM predicted material effects are compared with the results from the M-K analysis. The M-K analysis is carried out by a numerical method provided by Lian *et al.*[34]

A typical FLD on the positive minor strain regime may be assumed to be well represented by the following two quantities:[35,36] (1) the plane strain intercept, FLD_0 and (2) the shape of the FLD represented approximately by

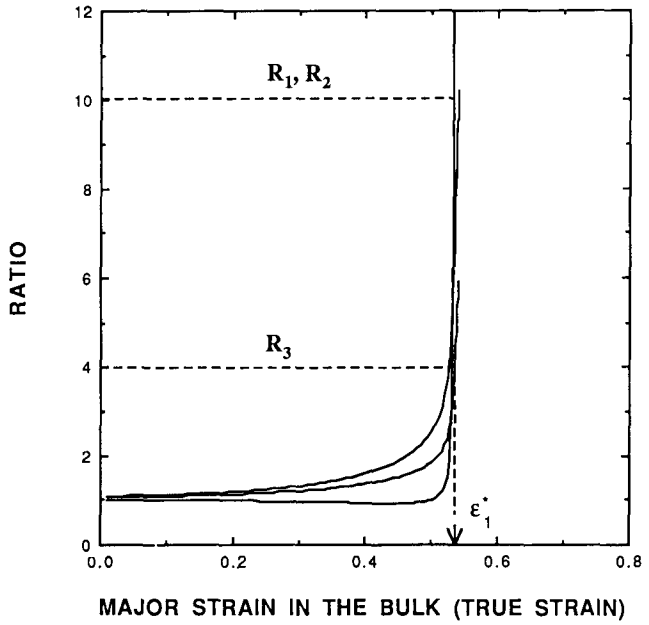

Fig. 4—Prediction of localized necking by major strain criterion, minor strain criterion, and effective strain criterion.

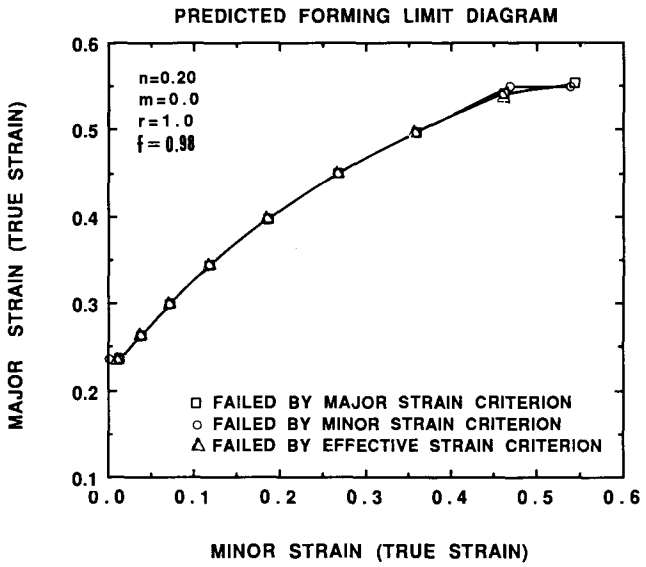

Fig. 5—FLDs based on the three failure criteria of Fig. 4.

a line. As suggested by Lian *et al.*[35] and Graf and Hosford,[36] it is convenient to separate the influence of material parameters on the FLD_0 and FLD shape.

A. *Effect of Material Parameters on the FLD_0*

Finite element modeling and M-K predictions, based on Hill's yield function ($M = 2$), are shown in Figure 6. The weakness factor, f, is assumed to be equal to 0.98. Figure 6(a) shows the sensitivity of the FLD_0 on the work-hardening exponent, n. It is seen that both FEM and M-K analysis predict a linear increase in the FLD_0 with an increase in n. This trend is in agreement with the previous results reported in the literature.[37,38,39] The sensitivity can be approximately quantified as the slope of the linear regression line in Figure 6(a). The FEM predicted sensitivity of the FLD_0 with n is equal to 1.04 and the corresponding sensitivity as predicted by M-K analysis is equal to 0.88.

Figure 6(b) shows the predicted near-linear dependence of the FLD_0 on the strain rate sensitivity index, m. The FEM predicted sensitivity of the FLD_0 with m is equal to 6.1 and the corresponding sensitivity predicted by M-K analysis is equal to 4.1.

The anisotropy parameter, r, does not produce a change in the predicted FLD_0 (Figure 6(c)). Both FEM and M-K analyses predict a zero sensitivity of the FLD_0 with r. This effect of r on the predicted FLD_0 has been explained by Sowerby and Duncan[39] based on the effect of r on the shape of the yield locus.

B. *Effect of Material Parameters on the FLD Shape*

As mentioned before, the shape of FLDs is approximately represented by a line. The strain ratio, ρ, for a strain path is equal to $\varepsilon_2/\varepsilon_1$. Lian *et al.*[35] and Graf and Hosford[36] used an average slope to represent the shape of an FLD. In Reference 36, the average slope is defined in the following manner:

$$\text{Average slope} = \frac{\varepsilon_1^*(\rho = 0.8) - \varepsilon_1^*(\rho = 0.2)}{\varepsilon_2(\rho = 0.8) - \varepsilon_2(\rho = 0.2)} \quad [9]$$

where $\varepsilon_1^*(\rho = 0.8)$ is the limiting true major strain in the predicted FLD when the strain ratio, ρ, is equal to 0.8, $\varepsilon_1^*(\rho = 0.2)$ is the limiting true major strain in the predicted FLD when the strain ratio, ρ, is equal to 0.2, and the ε_2's are the corresponding true minor strains. In this work, we approximate the FLD shape by a linear regression line passing through the predicted discrete points in the FLD (with $0.2 \leq \rho < 0.8$). We use the following ratio, P, to represent the shape of the FLD for our sensitivity analysis:

$$P = \frac{\varepsilon_1^*(\rho = 0.8)}{\varepsilon_1^*(\rho = 0.2)} \quad [10]$$

The above ratio is obtained from the linear regression line representing the FLD. The effect of material parameters of the FLD shape can now be evaluated as the effect of material parameters on the ratio P.

Figure 7 shows the predicted variation of P with an increase in the work-hardening exponent, n. The ratio P

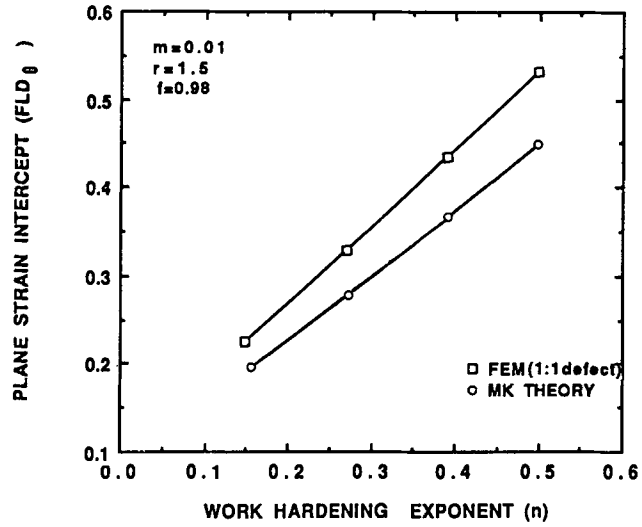

(*a*)

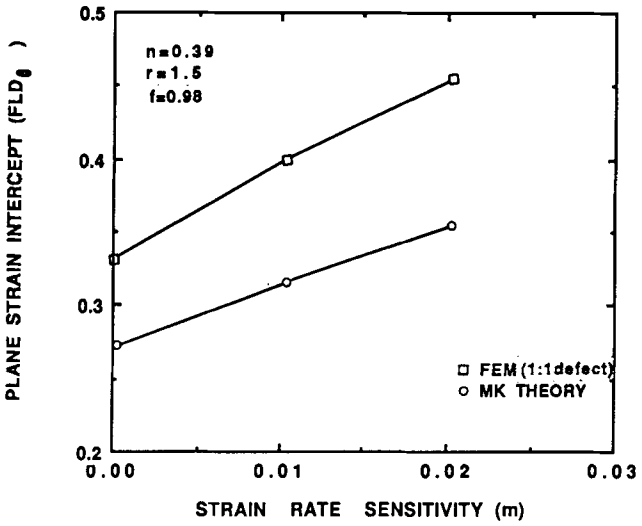

(*b*)

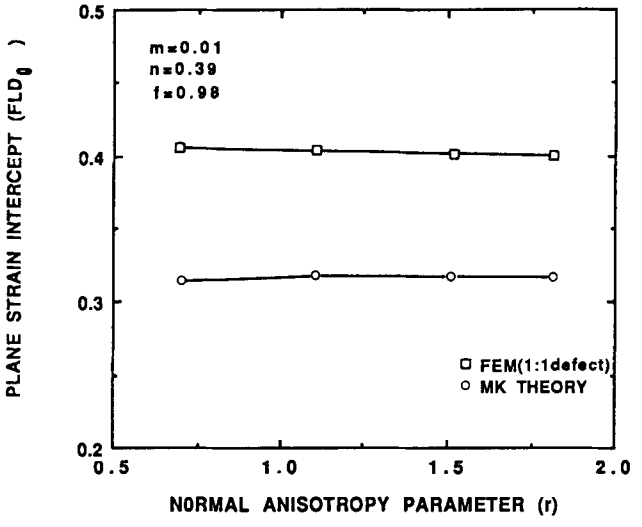

(*c*)

Fig. 6—The effect, at constant f, of the material properties on the simulated FLD_0: (*a*) work-hardening exponent, n, (*b*) strain rate sensitivity index, m, and (*c*) anisotropy index, r.

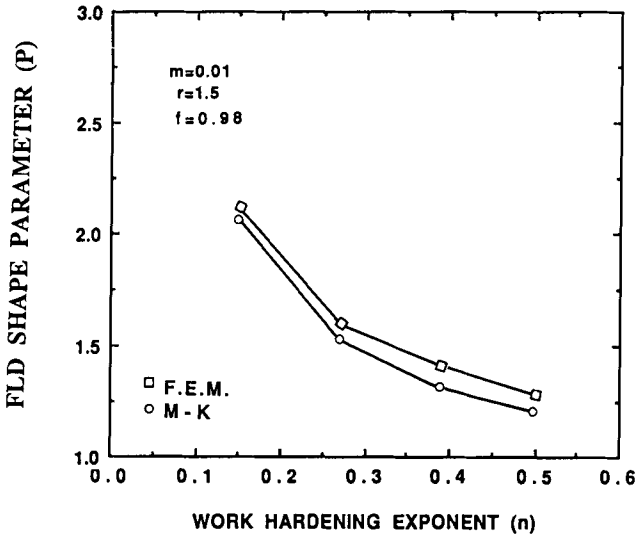

Fig. 7—The effect, at constant f, of the work-hardening exponent, n, on P (FLD shape parameter, see text).

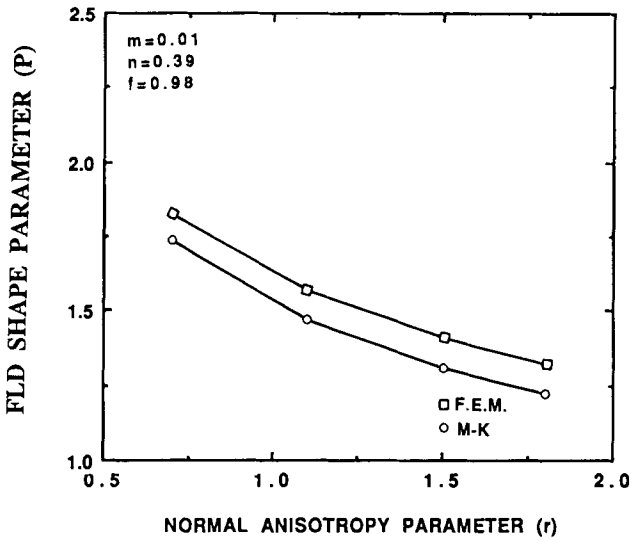

Fig. 9—The effect, at constant f, of the anisotropy parameter, r, on P (FLD shape parameter, see text).

decreases with increasing n, implying that the predicted limit strains are less dependent on the degree of biaxiality for larger magnitudes of n. The sensitivity of P to n may be approximated as the slope of the line in Figure 7. The sensitivity, as predicted by FEM, is equal to -2.33 and, as predicted by M-K analysis, is equal to -2.41.

Figure 8 shows the effect of the strain rate sensitivity index, m, on the ratio P. A small change in m produces a significant change in P, although the overall change in P is small for the range of m considered. The sensitivity of P to m is estimated as the slope of the line in Figure 8, which is equal to -10.5 as predicted by FEM analysis and is equal to -8.3 as predicted by the M-K analysis.

Figure 9 presents the effect of the anisotropic index, r (using Hill's yield function), on the shape of the FLD. For lower magnitudes of r, the ratio P is very sensitive to r. For larger magnitudes of r, the value of P becomes rather insensitive to r. The predicted influence of r on the FLDs is also dependent on the yield theory used. Many of the yield theories that have been developed recently to better describe the constitutive behavior of materials[35,36,40–42] show that r has no influence on the predicted FLDs. Figure 10 shows the predicted FLDs for a range of r values incorporating Hosford's yield theory by both FEM and M-K analyses. This result confirms the observations of previous researchers.[35,36,40–42] The above results show clearly that the effect of r on the FLD shape is very dependent on the assumed yield theory.

The effect of anisotropy, r, on the FLD shape has been explained by Lian *et al.*[35] by introducing a novel diagram called the *yield surface shape hardening diagram.*

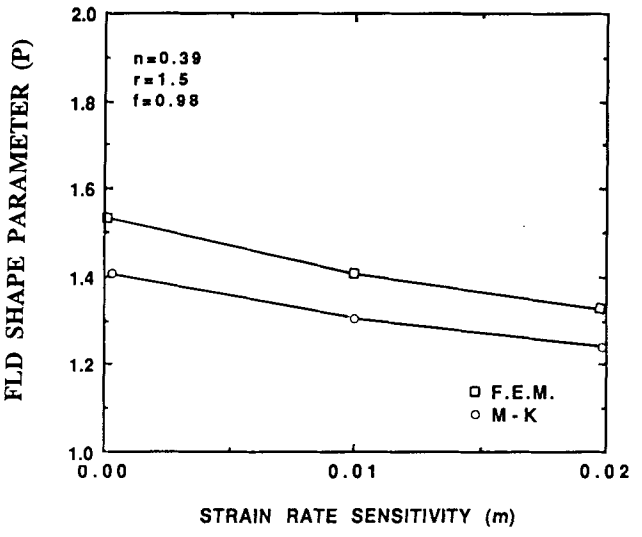

Fig. 8—The effect, at constant f, of the strain rate sensitivity index, m, on P (FLD shape parameter, see text).

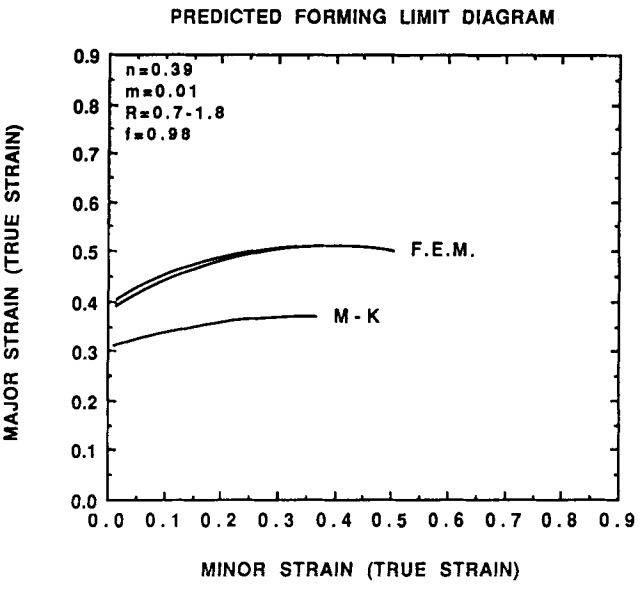

Fig. 10—The effect, at constant f, of the anisotropy parameter, r, on the predicted FLD using Hosford's yield theory by FEM and M-K.

The horizontal coordinate of this diagram is the strain path, $\rho(=\dot{\varepsilon}_{yy}/\dot{\varepsilon}_{xx})$, and the vertical axis is the ratio of the corresponding biaxial flow stress to the balanced biaxial flow stress (σ_{xx}/σ_b). They have shown that even though the plane stress yield surface shapes are different for different r values, the corresponding yield surface shape hardening diagrams are very similar, giving rise to similar FLDs. Therefore, they[35] have concluded that differences in predicted FLDs arise from differences in the corresponding yield surface shape hardening diagrams.

C. *Comparison of FEM and M-K Analyses*

A similar trend in the effect of material properties (n, m, and r) on the FLD (both the FLD_0 and shape) is predicted by both FEM and M-K analyses. Finite element modeling predicts larger magnitudes of FLD_0 and P (for a given weakness factor, $f = 0.98$) for all of the tested combinations of material parameters. For $f = 0.98$, the FLD_0's computed by FEM are on average 25 pct larger than those computed by M-K analysis. This is an expected result as the assumed M-K defect is more severe for a given sheet thickness than the defect assumed in the FEM analysis and hence would localize plastic deformation earlier. FEM predicted P values are slightly larger (on average by 8 to 10 pct) than those predicted by the M-K analysis. The higher magnitude of P predicted by FEM may be caused by the resulting larger FLD_0 rather than a real difference in the model. In order to investigate the role of the FLD_0 on P, the weakness factor of an M-K defect was varied for a given combination of material parameters (n, m, and r) and the corresponding FLD_0 and P were calculated. Figure 11 shows the variation of P with respect to the FLD_0. This result suggests that for any combination of material properties, the ratio P increases with the FLD_0. Therefore, it appears that the *shape* of the FLD (represented here simply by P) depends not only on n, m, and r, but also on the FLD_0, the formability of the material itself. (Of course, the FLD_0 may well be considered as a material property, but we distinguish between continuum plasticity properties like n, m, and r and the failure limit represented by the FLD_0).

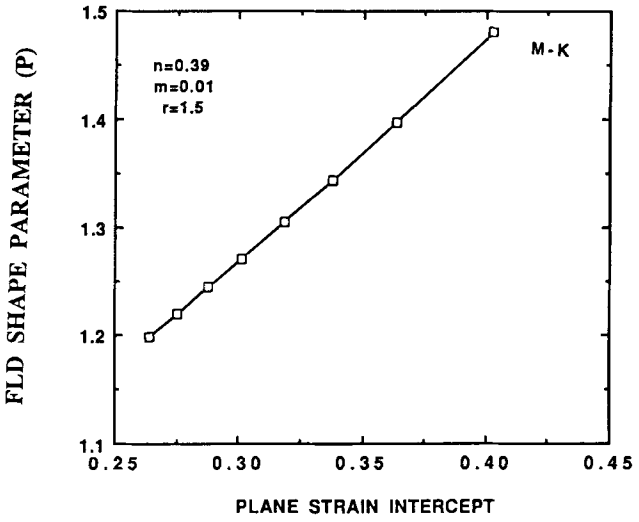

Fig. 11—The calculated variation of the ratio P (FLD shape parameter, see text) with the FLD_0 using M-K analysis.

For comparison with the work of previous researchers, we have so far compared FLDs computed using constant f values and notch geometries. As mentioned earlier, there appears to be no physical reason to do so, since f and notch geometry are unknown for real materials (worse, their origin or corresponding physical quantities have not been unambiguously identified). Therefore, the weakness factor, f, is merely a fit parameter convenient for normalizing a given model to the physical situation. It seems more instructive to us to compare the predicted FLDs for a given FLD_0, which is the experimentally determined quantity. The weakness factor must, therefore, be adjusted to achieve the specified FLD_0 with the specified material properties. For example, to obtain the FLD_0 that was obtained by M-K analysis (with $f = 0.98$), a weakness factor of $f = 0.935$ must be used in the FEM analysis (with 1:1 defect). The weakness factor required in FEM to predict the same FLD_0 obtained in M-K analysis is defined as f_{fem}.

Figure 12 compares the predicted FLDs computed from M-K analysis ($f = 0.98$) with ones computed by FEM analysis ($f = f_{fem} = 0.935$ and $f = 0.98$). The material properties are assigned various values for this comparison: $n = 0.15$ or 0.39, $m = 0.01$ or 0.02, and $r = 0.7$ to 1.5. Table I presents the pertinent P values for these simulations. The result is perhaps surprising and interesting in two regards.

(1) The shapes of M-K and FEM FLDs are nearly identical for a given n, m, r, and FLD_0, except very near the balanced-biaxial region. Bate and Wilson[15] showed similar results in their comparison for FEM analysis of a sheet containing interacting axisymmetric finite defects.
(2) The f_{fem} required in the FEM simulation to achieve the same FLD_0 as predicted by M-K analysis (for the same n, m, and r) does not depend on the material parameters n, m, or r, at least in the ranges tested in this work. The severity of the defect was shown not to have any influence on the required f_{fem} by Bate and Wilson.[15] These results imply that the f_{fem} required depends only on the starting geometry of the finite defect and does not depend on either the material properties or the severity (*i.e.*, thickness) of the assumed defects.

While the relationship between the f values required in the M-K and FEM analyses to obtain a specified FLD_0 does not depend on either plasticity properties or relative defect severity, it does clearly depend on the geometry of the assumed notch. The dependence of required f_{fem} on the aspect ratio of the notch is shown in Figure 13. For a larger aspect ratio, perhaps greater than 1:20, the FEM and M-K simulations would be nearly equivalent. Wilson and Ascelrad[43] have demonstrated similar results in a systematic set of experiments where they tested sheet materials with different defect lengths corresponding to different aspect ratios in the present FEM analysis. Burford and Wagoner[32] demonstrated the role of the defect aspect ratio in determining the FLD_0. Figure 14 shows the near correspondence between the FEM and M-K calculations when a large aspect-ratio notch (1:16) is employed. In this case, to match the FLD_0's, the requisite f values are 0.98 for M-K and 0.973 for FEM. The above

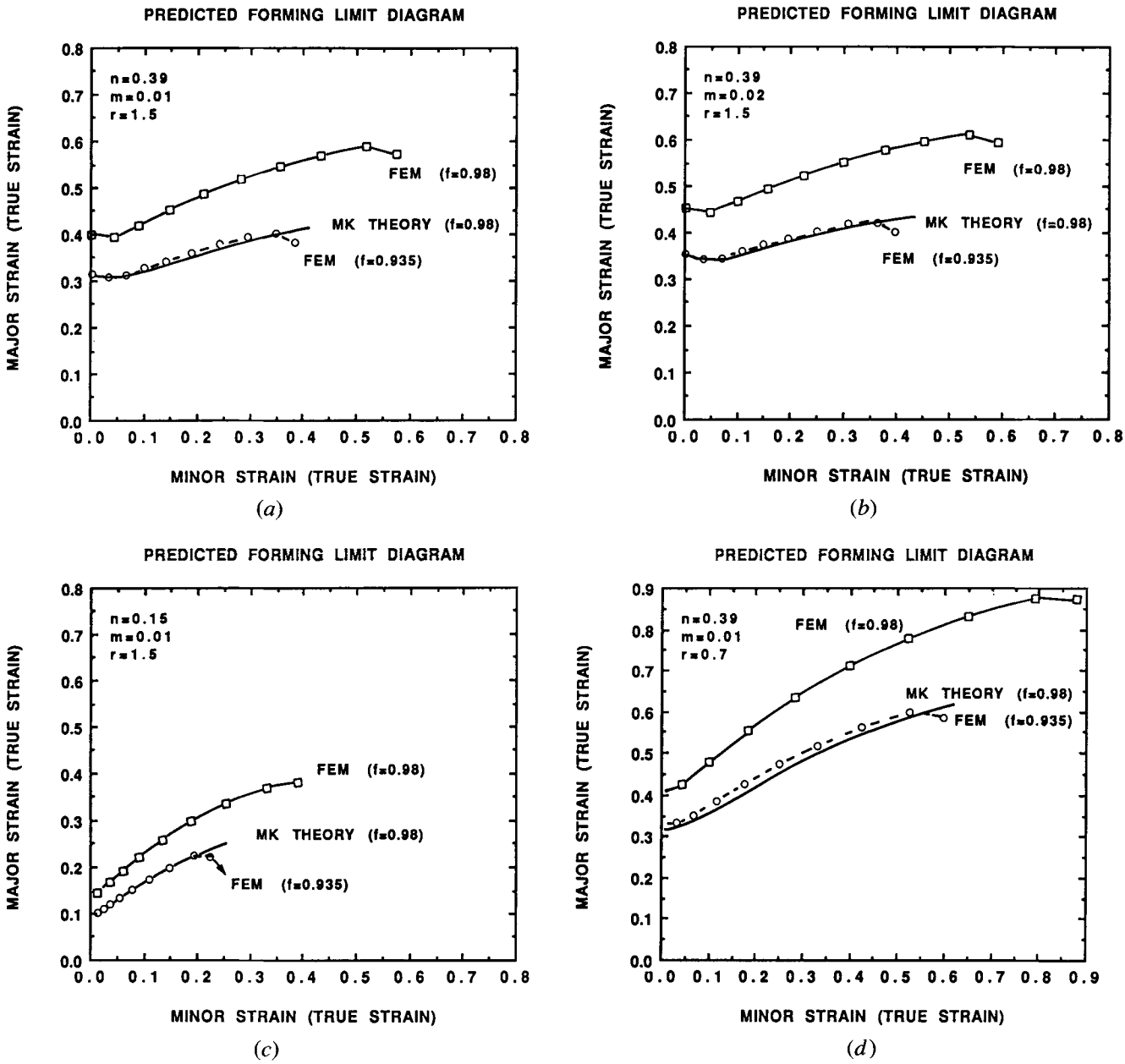

Fig. 12—Comparison of the predicted FLDs by M-K and FEM using constant f and required f_{fem}: (*a*) through (*d*) show the comparisons for different combinations of material properties.

results show that the f required in a theoretical model to match with an *experimental* FLD_0 depends not only on the continuum material properties (n, m, and r), but also on the assumed notch geometry and boundary conditions.

V. DISCUSSION

In the first part of the presented simulations, we followed the usual procedure of selecting model parametric values (n, m, r, and f) and used these values to compute FLDs. We did this using both M-K and FEM analyses and compared the two results. We found that there was little correspondence of the curves, their minimum values, or their shapes, Detailed results were presented under these conditions. As previous researchers reported, each of these parameters affects the height and shape of the FLD under these simulation rules, although the role of

Table I. Comparison of the Predicted Magnitudes of *P* for Different Material Property Combinations Before and After Matching the FLD_0's

	P		
Material Properties	FEM Before Matching the FLD_0	FEM After Matching the FLD_0	M-K
n = 0.15, m = 0.01, and r = 1.5	2.12	2.07	2.06
n = 0.39, m = 0.01, and r = 1.5	1.40	1.30	1.30
n = 0.39, m = 0.02, and r = 1.5	1.32	1.24	1.24
n = 0.39, m = 0.01, and r = 0.70	1.83	1.73	1.74

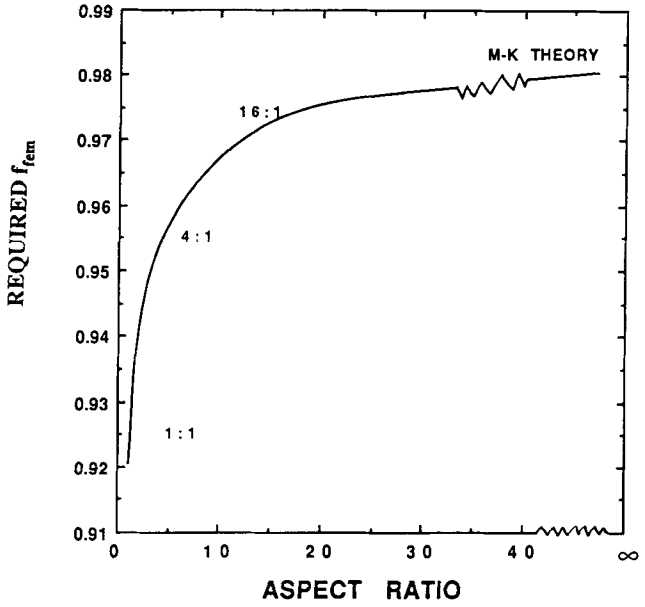

Fig. 13—The effect of the aspect ratio of the notch on the required f_{fem} (needed to match the FLD_0 predicted by M-K using $f = 0.98$).

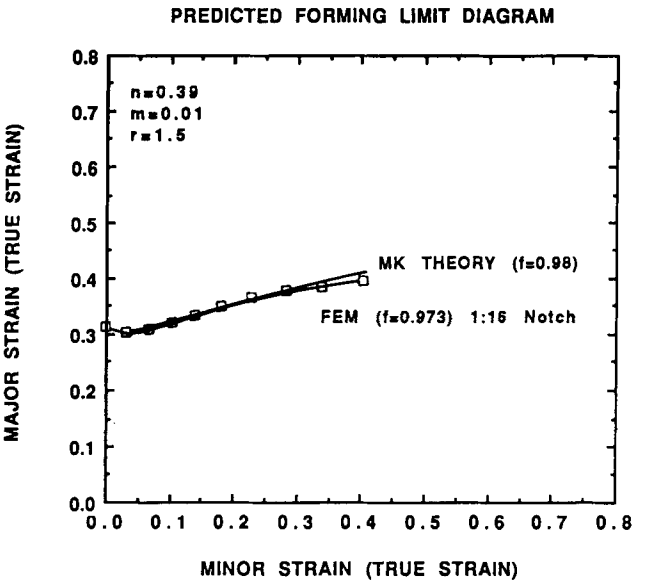

Fig. 14—Comparison of the predicted FLDs by M-K and FEM using a 1:16 aspect ratio notch and required f_{fem}.

the r value depends on the choice of plastic yield function; Hill's yield function (with $M = 2$) produces a strong r dependence while several other yield functions[35,36,40–42] do not. In all cases, the FEM calculation showed a higher forming limit than the M-K calculation, because the finite defect is less deleterious for a given weakness factor, f. The same trend was also found by Bate and Wilson[15] in their FEM analysis of sheet containing finite, interacting, axisymmetric defects. Previous work by Burford and Wagoner,[32] along with Figure 3, supports this reasoning. In fact, as the aspect ratio of the FEM notch approaches values in the range of 1:20, the FEM results approach the M-K ones, as also observed in the detailed experiments conducted by Wilson and Ascelrad.[43]

The underlying assumption in the foregoing discussion is that the parametric set (n, m, r, and f) is physically measurable and thus has meaning external to the simulation model. In fact, the subset (n, m, and r) satisfies this condition, but the parameter f does not. Although numerous attempts have been made to reconcile the M-K parameter, f (they conceived it as a pure thickness ratio), with various spatial variations of physical properties or variables (thickness, grain orientation, yield stress, temperature, *etc.*), it remains very much an arbitrary quantity introduced to allow M-K analyses to proceed. Finite element calculations[21,22] have shown that even mathematically homogeneous sheets (within the discreteness of the elements) are subject to consistent strain localization initiated by the usual frictional and geometric constraints found in actual forming operations. (It is only by chance that in-plane deformation under uniform boundary conditions, such as those envisaged by M-K, can proceed uniformly). Therefore, it appears hopeless to assign a physical meaning to f independent of the model used for calculating the FLD.

In Section IV–C of this article, we proposed to replace the nonphysical parameter f with the experimentally measured forming limit at the plane-strain condition, FLD_0. The corresponding set of pertinent parameters that affect the shape of the FLD then becomes (n, m, r, and FLD_0). Note that in this context, although the FLD_0 is used as a parameter independent of n and m, it is important to realize that FLD_0 itself (at constant defect shape, for example) strongly depends on both n and m. This approach implies that the FLD_0 should be experimentally measured and used along with n and m to predict the shape of the FLDs. While the FLD_0 is by no means an easy-to-measure or consistently obtainable quantity, it at least has a physical meaning defined by various kinds of sheet formability tests. We choose to interpret the FLD_0 as a measure of the material formability in plane-strain tension, which depends on the nature of the test, material continuum behavior, and perhaps, flaw content and sensitivity.

In a rather idealized comparison, the FLD_0 plays the role of the critical stress intensity factor in fracture mechanics tests. As for the case of fracture mechanics, there is always a need for a parameter to represent, in an average sense, the roles of continuum and noncontinuum contributions to failure. By collecting such parameters in a physically significant way, one can proceed to predict real failures which depend not only on material properties, but also on boundary conditions and defect distributions. This usage does not violate the common observation that the FLD_0 or K_{Ic} depends on material properties (n, m, and r, for example).

Using the FLD_0 as a basic material/test/geometric property, some of the FEM FLD simulations of the Section I were repeated with the FLD_0 held constant. The results provide a much more orderly and revealing comparison with respect to the M-K results. First, the shapes of the FLDs computed from FEM and M-K are nearly identical, implying that the results are not model-dependent as long as FLD_0 is chosen independently. The only exception appears to be near the balanced-biaxial symmetry line, where the FEM results often show a reduced slope, similar to some experimental results.[44–47]

Second, the relationship between the weakness factors required between the two models does not seem to vary with other material properties. That is, for the range of material properties tested, an $f = 0.98$ (M-K) appears to be equivalent to an $f = 0.935$ (FEM with 1:1 defect). It is rather surprising that the two models would not be more different in the way various material parameters interact to produce the final FLD.

With the adoption of the FLD_0 as a specified parameter in the simulations, it becomes clear that the "predictions" of the FLD_0 by various models are not physically motivated predictions at all. Rather, the model in question should be evaluated for shape of the predicted FLD (in comparison with the experimental one) at a specified, and fit, FLD_0.

VI. CONCLUSIONS

Forming limit diagrams have been computed using M-K 1-D analysis and 2-D FEM for a range of material properties. The FEM results were based on a notch of 1:1 aspect ratio with remote displacement boundary conditions. The following conclusions were reached.

1. At a given weakness factor (thickness of notch/thickness of bulk), f, FEM FLD_0's are 20 to 25 pct higher than M-K FLD_0's for all choices of material properties. Finite isolated defects are, therefore, less deleterious (at a given weakness factor) than the infinite channel M-K defects.
2. At a given weakness factor, f, the shape of the FLDs computed by the two methods are different because of the FLD_0 differences.
3. The shape of FLDs at a constant weakness factor, f, depends strongly on material strain hardening and strain rate sensitivity, but the role of the r value depends on choice of yield function, as found by previous researchers.[35,36,40–42]
4. The weakness factor, f, was interpreted to be not a physical quantity but rather a simulation parameter of little interest in comparison with physical FLDs.
5. The plane-strain forming limit, FLD_0, was proposed to replace the role of the weakness factor, f, in simulations and comparisons with experiments.
6. With the FLD_0 held constant, the shapes of FEM FLDs and M-K FLDs are nearly indistinguishable for a wide range of material properties. The FEM FLDs often show a maximum near the balanced-biaxial limit that does not appear in the M-K FLDs.
7. With the FLD_0 held constant, a constant relationship between the simulation weakness factors for the FEM and M-K simulations was found. The M-K defect with a weakness factor of $f = 0.98$ corresponded to the FEM 1:1 defect with a weakness factor of $f = 0.935$. This relationship depends only on the aspect ratio of the FEM defect and not on the material parameters.

ACKNOWLEDGMENTS

This work was jointly sponsored by The Edison Materials Technology Center, of Kettering, OH, and by the NSF Engineering Research Center for Net Shape Manufacturing, The Ohio State University. The use of the CRAY was made possible by a grant from the Ohio Supercomputer Center. The authors wish to thank Dr. D.A. Burford and Mr. D. Zhou for useful discussions.

REFERENCES

1. S.P. Keeler and W.A. Backofen: *ASM Trans. Q.*, 1964, vol. 56, pp. 25-48.
2. S.P. Keeler: Society of Automotive Engineers Technical Paper No. 650535, 1965.
3. S.P. Keeler: Sc.D. Thesis, Massachusetts Institute of Technology, Cambridge, MA, 1961.
4. G.M. Godwin: Society of Automotive Engineers Technical Paper No. 680093, 1968.
5. S.S. Hecker: *Sheet Metal Forming and Formability*, Proc. 7th Biennial Cong. of International Deep Drawing Research Group, Hoogovens Ijmuiden Bv, Amsterdam, Holland, 1972, pp. 5.1-5.8.
6. M. Azrin and W.A. Backofen: *Metall. Trans.*, 1970, vol. 1, pp. 2857-65.
7. *Forming Limit Diagrams: Concepts, Methods, and Applications*, R.H. Wagoner, K.S. Chan, and S.P. Keeler, eds., TMS, Warrendale, PA, 1989.
8. R. Hill: *J. Mech. Phys. Solids*, 1952, vol. 1, pp. 19-30.
9. Z. Marciniak and K. Kuczynski: *Int. J. Mech. Sci.*, 1967, vol. 9, pp. 609-20.
10. Z. Marciniak, K. Kuczynski, and T. Pokora: *Int. J. Mech. Sci.*, 1973, vol. 15, pp. 789-805.
11. K.S. Chan: in *Forming Limit Diagrams: Concepts, Methods, and Applications*, R.H. Wagoner, K.S. Chan, and S.P. Keeler, eds., TMS, Warrendale, PA, 1989, pp. 73-110.
12. *Mechanics of Sheet Metal Forming*, D.P. Koistinen and N.M. Wang, eds., Plenum Press, New York, NY, 1978.
13. P.B. Mellor: *Int. Met. Rev.*, 1981, vol. 26, pp. 1-20.
14. F.A. Nichols: *Acta Metall.*, 1980, vol. 28, pp. 663-73.
15. P. Bate and D.B. Wilson: *Int. J. Mech. Sci.*, 1984, vol. 26, pp. 363-72.
16. R.A. Ayres, W.G. Brazier, and V.F. Sajewski: *J. Appl. Metalworking*, 1979, pp. 41-49.
17. K. Chung and R.H. Wagoner: *Int. J. Mech. Sci.*, 1987, vol. 29, pp. 45-59.
18. N.M. Wang: in *NUMIFORM*, J.F.T. Pittman, R.D. Wood, J.M. Alexander, and O.C. Zienkiewicz, eds., Pineridge Press, Swansea, U.K., 1982, pp. 797-806.
19. K. Chung and R.H. Wagoner: *Metall. Trans. A.*, 1986, vol. 17A, pp. 1001-09.
20. K. Chung and R.H. Wagoner: *Metall. Trans. A.*, 1988, vol. 19A, pp. 293-300.
21. Y. Germain, K. Chung, and R.H. Wagoner: *Int. J. Mech. Sci.*, 1989, vol. 31, pp. 1-24.
22. J.R. Knibloe and R.H. Wagoner: *Metall. Trans. A*, 1989, vol. 20A, pp. 1509-21.
23. Y.H. Kim and R.H. Wagoner: *Int. J. Mech. Sci.*, 1987, vol. 29, pp. 179-94.
24. Y.H. Kim and R.H. Wagoner: *Scripta Metall.*, 1987, vol. 21, pp. 223-28.
25. Y.H. Kim and R.H. Wagoner: The Ohio State University, Columbus, OH, unpublished research, 1990.
26. R. Hill: *Math. Proc. Camb. Phil. Soc.*, 1979, vol. 85, pp. 179-91.
27. W.F. Hosford: *7th North American Metalworking Research Conf. Proc.*, Society of Manufacturing Engineers, Dearborn, MI, 1979, pp. 191-97.
28. R. von Mises: *Gottinger Nachr. Math. Phys. Klasse*, 1913, p. 582.
29. R. Hill: *Proc. R. Soc. London*, 1948, vol. 193A, pp. 281-97.
30. D. Zhou and R.H. Wagoner: The Ohio State University, Columbus, OH, unpublished research, 1989–1990.
31. R.W. Logan and W.F. Hosford: *Int. J. Mech. Sci.*, 1980, vol. 22, pp. 419-30.
32. D.A. Burford and R.H. Wagoner: in *Forming Limit Diagrams: Concepts, Methods, and Applications*, R.H. Wagoner, K.S. Chan, and S.P. Keeler, eds., TMS, Warrendale, PA, 1989, pp. 167-82.

33. R.W. Logan, D.J. Meuleman, and W.F. Hosford: in *Formability and Metallurgical Structure*, A.K. Sachdev and J.D. Embury, eds., TMS, Warrendale, PA, 1986, pp. 159-73.
34. J. Lian, D. Zhou, and B. Baudelet: *Int. J. Mech. Sci.*, 1989, vol. 31, pp. 237-47.
35. J. Lian, F. Barlat, and B. Baudelet: *Int. J. Plast.*, 1989, vol. 5, pp. 131-47.
36. A. Graf and W.F. Hosford: *Metall. Trans. A*, 1990, vol. 21A, pp. 87-94.
37. K.S. Chan, D.A. Koss, and A.K. Ghosh: *Metall. Trans. A*, 1984, vol. 15A, pp. 323-29.
38. D. Lee and F. Zaverl: *Int. J. Mech. Sci.*, 1982, vol. 22, pp. 157-73.
39. R. Sowerby and J.L. Duncan: *Int. J. Mech. Sci.*, 1971, vol. 13, pp. 217-29.
40. F. Barlat and O. Richmond: *Mater. Sci. Eng.*, 1987, vol. 95, pp. 15-29.
41. F. Barlat: *Mater. Sci. Eng.*, 1987, vol. 91, pp. 55-72.
42. A. Graf and W.F. Hosford: in *Forming Limit Diagrams: Concepts, Methods, and Applications*, R.H. Wagoner, K.S. Chan, and S.P. Keeler, eds., TMS, Warrendale, PA, 1989, pp. 153-63.
43. D.V. Wilson and O. Ascelrad: in *Proc. 10th IDDRG Meeting*, Warwick, U.K., Portcullis Press Ltd., Queensway House, Redhill, Surrey, U.K., 1978, pp. 155-66.
44. E. Schedin and A. Thuvander: *International Deep Drawing Research Group Working Group Meeting*, Schaffhausen, Switzerland, 1987.
45. D.N. Lee and Y.K. Kim: in *Forming Limit Diagrams: Concepts, Methods, and Applications*, R.H. Wagoner, K.S. Chan, and S.P. Keeler, eds., TMS, Warrendale, PA, 1989, pp. 37-59.
46. P. Bate: *Int. J. Mech. Sci.*, 1984, vol. 26, pp. 373-84.
47. S.S. Hecker: *J. Eng. Mater. Technol. Trans. ASME*, 1975, vol. 97H, pp. 66-73.